Paramagnetic Resonance and Optical Spectrum of Iron in Beryl*

M. Dvir and W. Low
Department of Physics, The Hebrew University, Jerusalem, Israel
(Received April 27, 1960)

The paramagnetic resonance spectrum of Fe^{3+} in beryl was measured at 20° and 290°K. In addition to this spectrum many weak lines were observed and possible explanations of these lines are discussed.

The optical spectrum shows a spectrum characteristic of trivalent iron. In the infrared region there are several groups of sharp lines whose origin is not yet known.

I. INTRODUCTION

THE paramagnetic spectrum of trivalent chromium in beryl was recently measured. A large initial splitting of 1.786 cm^{-1} was found.[1] This splitting of about 1.85 ± 0.2 cm^{-1} was confirmed from optical spectra.[2] It was of interest to see whether iron might give a splitting of comparable magnitude. Somewhat to our surprise it was found that the initial splitting is relatively small. In addition many weak lines were observed. Possible explanations for some of these absorption lines are given.

II. PARAMAGNETIC RESONANCE RESULTS

Crystallography

The structure of beryl has been investigated in detail.[3,4] Beryl grows in hexagonal crystals. There are 2 molecules $Be_3Al_2Si_6O_{18}$ per unit cell. Each aluminum ion is surrounded by six Si_6O_{18} rings. The nearest neighbors of each aluminum ion are six oxygen ions. The point symmetry of the aluminum ion is trigonal. The six oxygen ions form a squashed-in octahedron in which the distortion is along the 111 axis (the z axis). The oxygen-aluminum distance is 1.94 A. The separation between adjacent aluminum ions is 4.585 A and is parallel to the z axis. There are other aluminum ions at 5.64 A and 7.27 A, respectively. All aluminum ions are magnetically equivalent.

The beryllium ion is surrounded by a distorted tetrahedron of oxygen ions. Two oxygen ions lie nearly along one of the crystallographic "a" axes. There is a small rotation of about 9° from the "a" axis so that the lines connecting each two ion pairs make at their intersection an angle of about 102°. (The paramagnetic resonance data indicate that this angle may be about 97°.) The tetrahedron has a distortion along the z axis as if the cube is elongated parallel to the z axis. The Be-O distance is 1.73 A, and all Be ions are magnetically equivalent along this axis.

The silicon ion is surrounded by a nearly perfect tetrahedron. Along the z axis, the 100 direction of the cube containing the tetrahedron, the silicon ions are magnetically equivalent. The Si-O distance is 1.57 A.

Preliminary Discussion

The spectrum was scanned at room temperature and liquid hydrogen temperature at 3-cm wavelength. Natural aquamarine beryl crystals were used. These are transparent slightly bluish crystals showing clearly the cleavage planes. A spectral analysis indicated the presence of the following impurities: Zn$\sim$0.01%, Mg$\sim$0.1%, Fe$\gtrsim$0.1% and traces (0.001%) of Cr, Mn, Cu, Ti as well as a number of diamagnetic ions.

A cursory investigation showed 5 intense lines and many additional weaker lines stretching from nearly zero field up to 5000 gauss. The intensive lines showed an extreme separation along the z axis. At right angles to the axis the spectrum was isotropic. In the following we shall discuss the intense and weaker lines separately.

A. The Iron Spectrum in Octahedral Symmetry

The detailed measurements of the line position with $H\|z$, $H\perp z$ and $H\|[100]$ at room and liquid hydrogen temperature are given in Tables I and II. It is clear from the spectrum that the spin Hamiltonian can be expressed as a superposition of a cubic and axial contri-

TABLE I. Measured position of strong absorption lines at 290°K.

$H\|z$		$H\perp z$		$H\|[100]$	
Relative intensity	Magnetic field in gauss	Relative intensity	Magnetic field in gauss	Relative intensity	Magnetic field in gauss
85	2583	78	2707	20	2973.4
35	2635.3	165	3042	25	3107.7
110	3186.3	250	3161.3	125	3182
35	3736.9	···	3233.7	120	3327.5
85	3808.6	40	3603	240	3374.1
				175	3572.1
				20	3766.5
Free radical marker	3192.7		3150.9		3342.6

* This research was supported in part by the U. S. Air Force, Air Research and Development Command, through its European Office.

[1] J. E. Geusic, M. Peter, and E. O. Schulz-DuBois, Bell System Tech. J. 38, 291 (1959).

[2] W. Low (to be published).

[3] W. L. Bragg and J. West, Proc. Roy. Soc. (London) A111, 691 (1926).

[4] R. W. G. Wyckoff, *The Structure of Crystals* (The Chemical Catalog Company, New York, 1931).

TABLE II. Measured position of strong absorption lines at 20°K.

$H\|\|z$		$H\perp z$		$H\|\|[100]$	
Relative intensity	Magnetic field H in gauss	Relative intensity	Magnetic field H in gauss	Relative intensity	Magnetic field H in gauss
63	2642.2	20	2822	10	2826
28	2734.5	50	3167	8	2894.4
104	3238.8	100	3235	50	3047.8
34	3707.8	60	3290.5	80	3189.7
80	3839.4	20	3580.6	100	3237.1
			3598.4	6	3368.6
				50	3451
				10	3604.6
Free radical marker	3222.2		3215.3		3215.3

bution, i.e.,

$$\mathcal{H}=g\beta\mathbf{H}\cdot\mathbf{S}+B_2^0O_2^0+B_4^0O_4^0+(B_4^0)^*(O_4^0)^*+(B_4^4)^*(O_4^4)^*, \quad (1)$$

where O_n^m are the spin operators and B_n^m the crystal field parameters, or as expressed more conventionally:

$$\mathcal{H}=g\beta\mathbf{H}\cdot\mathbf{S}+(a/6)[S_\xi^4+S_\eta^4+S_\zeta^4-\tfrac{1}{5}S(S+1)(3S^2+3S-1)]+D[S_z^2-\tfrac{1}{3}S(S+1)]+(1/180)F[35S_z^4-30S(S+1)S_z^2+25S_z^2-6S(S+1)+3S^2(S+1)^2]. \quad (2)$$

Here the z axis is along the trigonal distortion, i.e., the [111] axis, and the ξ, η, ζ are the cubic axes.

The levels in zero field are given by direct diagonalization

$$W_{1,2}=\tfrac{1}{3}D-\tfrac{1}{2}(a-F)\pm\tfrac{1}{6}[(18D+a-F)^2+80a^2]^{\frac{1}{2}},$$
$$W_3=-\tfrac{2}{3}D+a-F. \quad (3)$$

The transitions corresponding to $\Delta M=\pm1$ can be evaluated by expanding the square root sign, assuming $g\beta H\gg a$, and are found to be[5]:

$$\begin{aligned}
\pm\tfrac{5}{2}\rightarrow\pm\tfrac{3}{2}\quad & H=H_0\mp[2D(3\cos^2\theta-1)+2pa+\tfrac{1}{6}Fq]-32\delta_1+4\delta_2+\epsilon_1,\\
\pm\tfrac{3}{2}\rightarrow\pm\tfrac{1}{2}\quad & H=H_0\mp[D(3\cos^2\theta-1)-\tfrac{5}{2}pa-(5/24)Fq]+4\delta_1-5\delta_2+\epsilon_2, \quad (4)\\
\tfrac{1}{2}\rightarrow-\tfrac{1}{2}\quad & H=H_0+16\delta_1-8\delta_2+\epsilon_3,
\end{aligned}$$

where $p=1-5\phi$, $\phi=l^2m^2+m^2n^2+l^2n^2$, $q=35\cos^2\theta-30\cos^2\theta+3$, and ϵ_i are terms of the order of (a^2/H_0), δ_i are terms of the order (D^2/H_0).

By taking separations of extreme lines for either $H\|z$ or $H\perp z$, i.e., $[M\rightarrow M-1][-(M-1)\rightarrow -M]$ one finds two equations in two unknowns D and $(a-F)$ which can be solved.

The values found for $H\perp z$, serve as a consistency check. The measurements along the [100] direction, however, yield two equations in two unknowns, a and F separately. Therefore these measurements are sufficient to establish the values and relative signs of D, a, and F. The g value is best found from the $\frac{1}{2}\rightarrow-\frac{1}{2}$ transition. Inspection of the relative intensities shows that along $H\|z$ the extreme lines belong to the $\pm\frac{3}{2}\rightarrow\pm\frac{1}{2}$ transitions whereas the inner pair belongs to the $\pm\frac{5}{2}\rightarrow\pm\frac{3}{2}$ lines. The evaluated constants in the spin Hamiltonian energy level separations are given in Table III. It is seen that the relative signs of D, a, and F are the same. From this table it is evident that adjacent lines have the same sign of $M\rightarrow M-1$. This enables us to establish the absolute sign at low temperature. It is found that the pair of lines at high field are of larger intensity. Therefore D must be positive, and similarly a and F.

Discussion

The most significant aspect is that the initial splitting of Fe^{3+} in beryl in considerably smaller than that found for Fe^{3+} in aluminum oxide or for Cr^{3+} in beryl. It is obvious, therefore, that there is no simple relationship between the strength of the axial perturbation and the initial splitting of the levels.

It is gratifying to find the sign $a-F$ and the cubic field parameter a positive, similarly to that found for many octahedral and tetrahedral compounds.[6] On the other hand, there seems to be a correlation as far as the sign of the parameters in the Hamiltonian is concerned. In both beryl and aluminum oxide the sign of D is negative for Cr^{3+} and positive for Fe^{3+}.

B. Weaker Lines

A large number of weaker lines is found which spread from low to high magnetic fields. The most prominent as determined at 20°K with $H\|z$ are listed in Table IV and are shown schematically in Fig. 1.

TABLE III. Calculated parameters of spin Hamiltonian at 20°K and 290°K.

Parameters at	a	D (in units of 10^{-4} cm^{-1})	F	$g_\parallel$	$g_\perp$	Energy levels in 10^{-4} cm^{-1} W_1	W_2	W_3
20°K	+153.2±1	+140.2±2	+10.8±3	1.998±0.002	2.002±0.002	476	−525	49
290°K	153.5±1	174.0±2.5	17.7±4	2.001±0.002	2.002±0.002	576	−595	18.7

[5] B. Bleaney and R. S. Trenam, Proc. Roy. Soc. (London) **A223**, 1 (1954).
[6] W. Low, *Paramagnetic Resonance in Solids* (Academic Press, New York, 1960).

These lines may be caused by a number of reasons. We list only the main possibilities:

(a) Forbidden transitions corresponding to $\Delta M = \pm 2, 3, 4, 5$. These fall in the low magnetic field region.

(b) Trivalent iron located either at the beryllium or silicon sites.

(c) Spectra caused by neighboring iron pairs. These nearest pairs would be along the z axis. This would give rise presumably to an additional interaction of the form $J\mathbf{S}_1\cdot\mathbf{S}_2$ and additional pseudodipolar terms. If J is large, as it is likely for iron, then $S=5, 3, 2, 1, 0$ would be good quantum numbers and give rise to relative complicated and temperature dependent spectra.

Note added in proof.—Since the closest distance between neighboring ions is about 4.5A it is likely that the exchange interaction J is small. We have observed (U. Rosenberger and W. Low) many additional lines in emerald probably caused by Cr—Cr pairs which seem to indicate that J is small there as well.

TABLE IV. Relative weak lines as measured at 20°K with $H||z$ axis. The magnetic field measurements is accurate to within 10 gauss. The relative intensity is only a qualitative measurement.

No.	Relative intensity	Magnetic field in gauss	No.	Relative intensity	Magnetic field in gauss
1	28	700	14	125	2940
2	50	980	15	250	3040
3	45	1115	16	250	3440
4	30	1350	17	150	3560
5	100	1800	18	180	3660
6	135	1990	19	125	3700
7	180	2130	20	50	4120
8	12	2450	21		4130
9	50	2520	22	10	4200
10	50	2570	23	10	4260
11		2580	24	15	4360
12	75	2750	25	170	4450
13	175	2840	26	65	4750
			27	40	5720

(d) Divalent iron situated at the site of beryllium in tetrahedral symmetry. The energy level scheme is somewhat complicated. However a few transitions between a number of singlets lie in the microwave region and could possibly be observed.

(e) Other unknown paramagnetic impurities. The optical spectra discussed below seem to indicate that other paramagnetic impurities may be present.

We shall discuss here only the first two possibilities. The other conjectures will be left for later investigations.

(a) Calculations of the transitions to $\Delta M=2, 3, 4, 5$ using the crystal field parameter given in Table III show that one can expect low field transitions as listed in Table V. This seems to account reasonably well for lines at low magnetic fields. These transitions are shown in Fig. 2.

(b) There are two sets each of four lines symmetrically located with respect to the strong $\frac{1}{2}\rightarrow-\frac{1}{2}$ transition which seem to behave somewhat differently from the others. We should like tentatively to ascribe one set of four levels to Fe^{3+} at the beryllium site and one set of lines to Fe^{3+} at the silicon site. From the nature of the width of the lines as well as the variation of the spectrum when the magnetic field is rotated with respect to the crystal axis it is indicative that one set of lines, that is to say lines Nos. 14, 15, 16, and 17 refer to one type of Fe^{3+} and another set of lines, Nos. 12, 13, 18, and 19 refer to another type of Fe^{3+}.

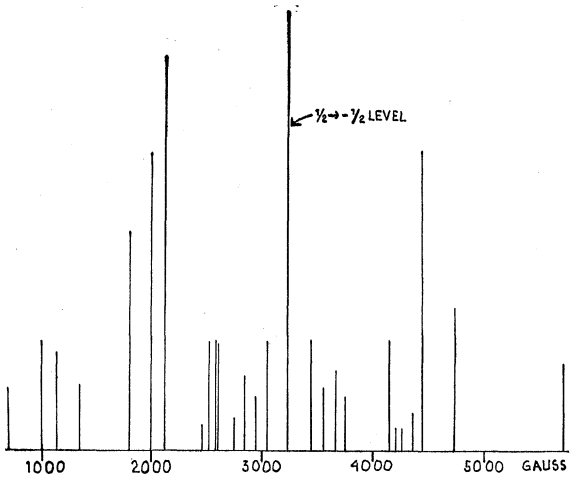

FIG. 1. The main weak lines as observed with $H||z$ at 3 cm wavelength at 20°K. The $\frac{1}{2}\rightarrow-\frac{1}{2}$ strong line (not drawn to scale) is shown as reference. The $\frac{1}{2}\rightarrow-\frac{1}{2}$ line is flanked by two sets of four absorption lines symmetrically displaced. These are discussed in the text.

We tentatively ascribe the first set of lines of larger intensity to iron at the beryllium site, assuming that the trivalent charge does not change the direction of the distortion of the tetrahedron. The reasons for this assignment are as follows. The Be—O distance is 1.73 A, whereas the Si—O distance is only 1.57 A. It is therefore likelier that Fe^{3+} with its large ionic radius will, if at all, be preferentially substituted at the beryllium site rather than at the silicon site. In addition the crystal field parameters calculated below show a large axial distortion whereas for the second set only a small distor-

TABLE V. Low level transitions calculated from the crystal field parameters (20°K) in Table IV.

	Transition	Approximate position H in gauss	Possible assignment of observed lines in gauss
$\Delta M=2$	$\frac{5}{2}\rightarrow\frac{1}{2}$	1120	980 or 1115
	$\frac{3}{2}\rightarrow-\frac{1}{2}$	1950	1990
$\Delta M=3$	$\frac{5}{2}\rightarrow-\frac{1}{2}$	750	700
	$\frac{3}{2}\rightarrow-\frac{3}{2}$	2090	2130
	$\frac{1}{2}\rightarrow-\frac{5}{2}$	1400	1350
$\Delta M=4$	$\frac{5}{2}\rightarrow-\frac{3}{2}$	750	700
	$\frac{3}{2}\rightarrow-\frac{5}{2}$	1380	1350
$\Delta M=5$	$\frac{5}{2}\rightarrow-\frac{5}{2}$	1130	980 or 1115

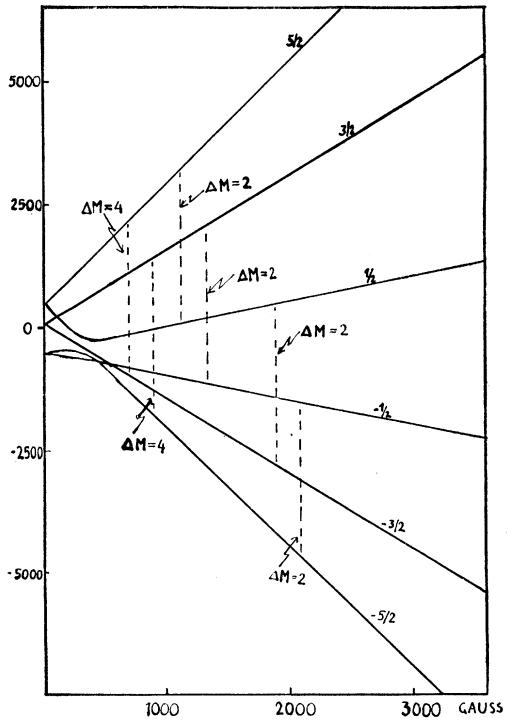

FIG. 2. Energy level scheme of Fe^{3+} in the octahedral symmetry of beryl. The low field "forbidden" transitions are indicated.

tion. As mentioned before the x-ray data indicate that the beryllium tetrahedron is distorted whereas the silicon tetrahedron is nearly undistorted.

Assuming this one can calculate for $H||z$, $\theta=90°$, $p=1$:

$$4D-2(a+\tfrac{1}{4}F)=\pm 400 \text{ gauss},$$
$$2D+\tfrac{5}{2}(a+\tfrac{1}{4}F)=\pm 620 \text{ gauss}.$$

Assuming that $a>\frac{1}{4}F$ and a to be positive as in all iron complexes, two of the four possible solutions can be discarded. Moreover assuming that a is proportional to the square of the crystal field potential,[7] then

$$a_{\text{oct}}/a_{\text{tet}}=(9/4)^2(d_{\text{tet}}/d_{\text{oct}})^{10}, \quad (5)$$

and the calculation gives a_{tet} as of the order of 104 gauss.

From the above we obtain two solutions:

$a+\frac{1}{4}F=109\pm 12$ gauss, $\quad a+\frac{1}{4}F=234\pm 12$ gauss,
$D=155\pm 7$ gauss, $\quad D=17\pm 7$ gauss.

Since F is presumably small the first solution is in better agreement with the expected cubic field parameter for tetrahedral symmetry.

Similar considerations prevail for the second set of four lines. Assuming this to belong to iron at a silicon site, then in this case $\theta=0$, $p=-\frac{3}{2}$. We find

$$a-(4/9)F=268\pm 12 \text{ gauss},$$
$$D=-2.0\pm 7.5 \text{ gauss},$$
$$a-(4/9)F=111\pm 12 \text{ gauss},$$
$$D=144\pm 7 \text{ gauss},$$

For the small tetrahedral radius a is expected to be of the order of 270 gauss. Also, the silicon tetrahedron is slightly distorted, and, therefore, the first solution is to be preferred.

At the best this interpretation is to be considered as a conjecture which needs more experimental evidence, such as could be obtained from the detailed measurements of the angular variation of these spectra. This is somewhat difficult experimentally because of the very strong and wide absorption lines of the Fe^{3+} situated at the aluminum sites.

III. THE OPTICAL SPECTRUM

The optical spectrum can be divided into two parts. Relatively weak and wide lines in the visible range which are apparently associated with the iron spectrum and stronger but fairly narrow lines in the infrared and red region.

TABLE VI. Measured absorption lines and possible assignment of energy levels of Fe^{3+} in an octahedral field.

Assigned transitions	Measured energy level
$^6A_1 \rightarrow {}^4F_1(d\epsilon^4 d\gamma)$	14 200 cm^{-1}
$^4F_2(d\epsilon^4 d\gamma)$	17 500 cm^{-1}
	20 000 cm^{-1}
$^4E(d\epsilon^3 d\gamma^2)$, $^4A_1(d\epsilon^3 d\gamma^2)$	23 600 cm^{-1}
$^4F_2(d\epsilon^3 d\gamma^2)$	26 500 cm^{-1}
$^4E(d\epsilon^3\gamma^2))$	27 300 cm^{-1}

In the visible region we have stronger lines at 23 600, 26 500 and 27 300 cm^{-1} and very weak absorption lines at 14 700, 17 500 and 20 000 cm^{-1}. These are transitions similar to those found by many authors for trivalent iron in octahedral complexes. Table VI gives a tentative assignment of the level scheme for these transitions. The assignment is made assuming the cubic field to be dominant. A reasonably large trigonal field may make some of these assignments uncertain, since the three-fold degenerate levels will split up with separations of at least a few hundred cm^{-1}.

The spectrum in the infrared is very rich in lines. The surprising feature is that even at room temperature some of these lines are very narrow (less than 10 cm^{-1}). In general the spectrum can be summed up as follows: There are four groups of strong lines, a number of lines at about 3500, 4500, 5300 and 7200 cm^{-1}. In addition there is a very intense and broad line at 12 300 cm^{-1},

[7] H. Watanabe, Progr. Theoret. Phys. Soc. (Kyoto) **9**, 753 (1954).

and a number of weaker lines. After heating the crystal in an atmosphere of H_2 there appeared another line at 7850 cm^{-1}.

We have no explanation of the spectrum in the infrared. We have tried to fit the spectrum to Fe^{2+} in tetrahedral symmetry. However the multiplicity of the lines and the narrowness seem to be indicative for transitions belonging to some rare earth or uranium group impurity.

ACKNOWLEDGMENT

We are grateful to Dr. E. Fischer of the Weizmann Institute of Science for permission to use the Cary spectrophotometer.

PHYSICAL REVIEW VOLUME 119, NUMBER 5 SEPTEMBER 1, 1960

Critical Fields of Thin Superconducting Films*

WILLIAM B. ITTNER, III
International Business Machines Research Laboratory, Poughkeepsie, New York
(Received April 25, 1960)

The critical fields of thin superconducting films have been calculated on the basis of the Bardeen-Cooper-Schrieffer (BCS) theory of superconductivity following a method outlined by Schrieffer. It is shown that it is convenient to use the critical field formula postulated by London where the London penetration depth is replaced by an effective penetration depth which can be specified through the use of the BCS theory. The effective penetration depth, unlike the London penetration depth which, for a given material, varies only with the temperature, is found to vary, in the BCS theory, with both the film thickness and the electronic mean free path of the normal material. This paper attempts to show that the measured critical fields of thin tin films are in general qualitative agreement with the predictions of the BCS theory.

INTRODUCTION

RECENT measurements carried out on thin superconducting tin films[1] have shown that the experimentally measured values of the externally applied longitudinal field required to destroy superconductivity are greater than would be expected on the basis of the London theory of superconductivity. This behavior has, indeed, been anticipated. Lutes,[2] in studying the critical fields of thin relatively impure tin whiskers, concluded that the superconducting penetration depths were considerably greater than the London value. Experiments by Schawlow[3] on several cylindrical tin films likewise indicated that the magnetic penetration depth in a superconductor will be a function, not only of the specimen purity, but of the specimen thickness as well. Likewise, Glover and Tinkham[4] found, in microwave measurements on thin films, that the effective penetration depth was increased appreciably over its value in bulk material.

These experimental results are, in fact, suggested by the various modern theories of superconductivity[5–7] which indicate that the supercurrent density is correctly expressed as an integral of the vector potential and will vary with both the specimen dimensions and the normal state electronic mean free path. As a consequence of this nonlocal aspect of superconductivity, the effective penetration depth (as it appears in the London theory) will be expected to depend on both the specimen dimensions and bulk mean free path. These considerations have been discussed by Tinkham[8] who suggested a practical method of treating the penetration depth to be used in the London theory. The results presented here are in qualitative agreement with the results outlined by Tinkham.

LONDON THEORY

It is instructive to carry out a number of calculations on the basis of the London theory of superconductivity to illustrate the general methods which are involved. Moreover, as the nonlocal theories are rather intractable in a mathematical sense, it will subsequently prove expedient to make use of a modified London equation where the London penetration depth, λ_L, is replaced by an effective penetration depth, λ_ϵ whose magnitude is indicated by the nonlocal theory.

In the London theory[9] the spatial variation of magnetic field, $H(x)$, inside a film of thickness d is

$$\frac{H(x)}{H_0}=\frac{\cosh x/\lambda_L}{\cosh d/2\lambda_L}, \tag{1}$$

* Supported, in part, by the Department of Defense.

[1] The films reported on in this work were fabricated and measured both by Mr. R. G. Blumberg of the IBM Federal Systems Division, Kingston, New York, and by Mr. A. E. Brennemann of the IBM Research Laboratory, Poughkeepsie, New York.

[2] O. S. Lutes, Phys. Rev. **105**, 1451 (1957).

[3] A. L. Schawlow, Phys. Rev. **109**, 1856 (1958).

[4] R. E. Glover and M. Tinkham, Phys. Rev. **104**, 844 (1956); **108**, 243 (1957).

[5] A. B. Pippard, Proc. Roy. Soc. (London) **A216**, 547 (1953).

[6] J. Bardeen, L. N. Cooper, and J. R. Schrieffer, Phys. Rev. **108**, 1175 (1957).

[7] N. N. Bogoliubov, Nuovo cimento **7**, 794 (1958).

[8] M. Tinkham, Phys. Rev. **110**, 26 (1958).

[9] H. London, Proc. Roy. Soc. (London) **A152**, 650 (1935).